J. Phys. B: At. Mol. Opt. Phys. **31** (1998) 1781–1792. Printed in the UK PII: S0953-4075(98)87100-9

Elastic cross sections for electron–ozone collisions

M T Lee†, S E Michelin‡, T Kroin† and L E Machado§

† Departamento de Química, Universidade Federal de São Carlos, 13565-905, São Carlos, SP, Brazil

‡ Departamento de Física, Universidade Federal de Santa Catarina, 88049, Florianópolis, SC, Brazil

§ Departamento de Física, Universidade Federal de São Carlos, 13565-905, São Carlos, SP, Brazil

Received 25 August 1997, in final form 15 December 1997

Abstract. We report a theoretical study of elastic electron–O_3 collisions in the 3–80 eV energy range. Calculations are carried out in a fixed-nuclei approximation at the ground-state equilibrium geometry of ozone. The Schwinger variational iterative method is used to calculate the low partial-wave scattering amplitudes at the static-exchange level whereas higher partial-wave contributions were taken into account through a Born-closure procedure using a point-dipole potential. The results presented are compared with available experimental and theoretical data in the literature and results are encouraging.

1. Introduction

From a chemical point of view, ozone is a very interesting molecule because it constitutes a unique known molecule in nature which presents a permanent dipole moment although formed by atoms of the same element. Moreover, despite the fact that ozone is only a minor constituent of the Earth's atmosphere, it plays an important role in controlling the Earth's thermal and radiation balances (Johnstone *et al* 1992). In particular, the presence of ozone in the upper atmosphere is essential to all life as it screens biologically harmful UV radiation (Shyn and Sweeney 1993). Also, electronic quenching and energy transfer involving ozone electronic states in the upper atmosphere can increase the excited-state populations of ozone and other atmospheric species and thereby perturb local thermodynamic equilibrium (Shyn and Sweeney 1993). To understand how ozone interacts chemically and physically in these systems a basic understanding of the properties of the ozone molecule itself is required. Information provided by electron–ozone scattering is also important to studies on the upper atmosphere. In addition, the study of electron–ozone collisions is important in electrical discharge for generating ozone (i.e. an ozonizer) as well (Eliasson *et al* 1983).

Because of these applications, it is not surprising that there has recently been increasing interest in the e^-–O_3 interactions. Some electron energy-loss spectra of ozone were reported by Celotta *et al* (1974), Swanson and Celotta (1975) and more recently by Johnstone *et al* (1992). Electron-impact ionization cross sections of ozone were reported by Siegel (1982). Also, measurements of elastic electron scattering cross sections for incident energies up to 20 eV were recently reported by Shyn and Sweeney (1993) and Allan *et al* (1996). On the theoretical side, although the electronic structure of O_3 molecule has been extensively studied (Mack and Muenter 1977, Andersson *et al* 1992, Maroulis 1992),

0953-4075/98/081781+12$19.50

very few investigations have been performed on the dynamic aspects of the molecule. To our knowledge, the only calculation of differential, integral and momentum-transfer cross sections for elastic e^-–O_3 collision in the 5–20 eV range was reported by Okamoto and Itikawa (1993). In their work, the authors employed an effective model potential in which the electrostatic potential is treated exactly and the electron exchange and target polarization are taken into account approximately by a local potential. The calculated differential cross sections (DCS) by Okamoto and Itikawa (1993) show some oscillations which are not seen in the measured data (Shyn and Sweeney 1993, Allan *et al* 1996). These oscillations may have resulted either by the lack of convergence in the partial-wave expansion for the wavefunction of the scattered electron, since they have truncated the expansions at $l = 8$, or by the Born-closure procedure used by these authors to take into account the contributions of higher angular-momentum components. As pointed out by Rescigno and Lengsfield (1992), the Born correction applied directly on the cross sections can actually lead to unphysical negative cross sections if the angular momentum expansion is too severely truncated. More recently elastic integral cross sections calculated at the static-exchange level for scattering energies below 20 eV were also reported by Sarpal *et al* (1994) using the *R*-matrix method. In that study, the authors have identified two shape resonances in both the A_1 (at 8.2 and 18.0 eV) and B_2 (at 11.1 and 18.1 eV) irreducible representations and also one resonance in the A_2 representation (at near 20 eV), although they have admitted that the resonances located at around 18–20 eV might be unphysical. Neither the measured data of Shyn and Sweeney (1993) nor the calculated results of Okamoto and Itikawa (1993) give evidence of such resonance structures. This is probably due to the fact that both calculations and measurements were carried out at a few sparsely distributed incident energies.

In this work, we report a theoretical study of the elastic electron scattering by ozone. More specifically, we calculate differential, integral and momentum-transfer cross sections in the 3–80 eV energy range. Our calculations are carried out in the fixed-nuclei approximation at the ground-state equilibrium geometry of O_3 at the static-exchange (SE) level in which both the electrostatic potential and the electron exchange effects are treated exactly. The Schwinger variational iterative method (SVIM) (Lucchese *et al* 1982) is used to calculate the low partial-wave scattering amplitudes at the SE level whereas higher partial-wave contributions were taken into account through the Born approximation with a point-dipole potential. In our earlier studies on electron scattering by polar molecules (Machado *et al* 1995a,b), we noted that the target polarization effects is relatively less important than the permanent dipole effects. Thus no polarization potential is included in this study. Different from the earlier calculation of Okamoto and Itikawa (1993), in this study the partial-wave expansion for the continuum wavefunctions were truncated at $l_c = 16$. Also the high angular-momentum contributions were included directly on the *T*-matrix through the prescription of Rescigno and Lengsfield (1992).

We expect that this study can contribute to the confirmation the existence of the shape resonances reported by Sarpal *et al* (1994) as well as clarifying the origin of the oscillations in the calculated DCS of Okamoto and Itikawa (1993). Also our calculated results for energies above 20 eV are presented for the first time in this work.

This paper is organized as follows. In section 2, we briefly describe the theory used and also some details of our calculation. Comparison between calculated results and available experimental and theoretical data will be presented in section 3.

2. Theory and calculation

In this section we will briefly discuss the method used; further details can be found elsewhere (Lucchese *et al* 1982, Machado *et al* 1995b). The laboratory-frame (LF) molecular orientation averaged differential cross sections (DCS) for elastic electron–molecule scattering is given by:

$$\frac{\mathrm{d}\sigma}{\mathrm{d}\Omega} = \frac{1}{8\pi^2}\int \mathrm{d}\alpha\ \sin\beta\,\mathrm{d}\beta\,\mathrm{d}\gamma\,|f(\hat{k}', \hat{k}_0')|^2 \tag{1}$$

where $f(\hat{k}', \hat{k}_0')$ is the LF scattering amplitude, $\hat{k}'$ and $\hat{k}_0'$ are the directions of scattered and incident electron linear momenta, respectively, and (α, β, γ) are the Euler angles which define the direction of the molecular principal axis. The LF-scattering amplitude $f(\hat{k}', \hat{k}_0')$ is related to the LF T-matrix elements by the formula

$$f(\hat{k}', \hat{k}_0') = -2\pi^2 T. \tag{2}$$

The Schwinger variational expression for the body-frame (BF) T-matrix elements can be written in the bilinear form

$$T^{(\pm)}_{\vec{k}_0,\vec{k}} = \langle \Phi^{(\mp)}_{\vec{k}} \mid U \mid \tilde{\Psi}^{(\pm)}_{\vec{k}_0}\rangle + \langle \tilde{\Psi}^{(\mp)}_{\vec{k}} \mid U \mid \Phi^{(\pm)}_{\vec{k}_0}\rangle\langle \tilde{\Psi}^{(\mp)}_{\vec{k}} \mid U - UG_0^{(\pm)}U \mid \tilde{\Psi}^{(\pm)}_{\vec{k}_0}\rangle \tag{3}$$

where $U(\vec{r}) = 2V(\vec{r})$ is the reduced interaction potential operator (in atomic units) between the target and the scattering electron, $\tilde{\Psi}^{(\pm)}_{\vec{k}}$ denote trial scattering wavefunctions with outgoing- (+) or incoming-wave (−) boundary conditions and $\Phi_{\vec{k}}$ and $G_0^{\pm}$ denote the free-particle wavefunction and Green operator, respectively. The trial scattering wavefunctions can be partial-wave expanded as:

$$\tilde{\Psi}^{(\pm)}_{\vec{k}}(\vec{r}) = \left[\frac{2}{\pi}\right]^{\frac{1}{2}}\frac{1}{k}\sum_{p\mu lh} \mathrm{i}^l\,\tilde{\Psi}^{(\pm)^{p\mu}}_{k,lh}(\vec{r})\,X^{p\mu}_{lh}(\hat{k}) \tag{4}$$

Table 1. Basis sets used for the trial scattering functions.

Scattering symmetry	Centre	Cartesian Gaussian function[a]	Exponents
ka_1	O_1	s	16.0, 8.0, 4.0, 2.0, 1.0, 0.5, 0.1
		z	4.0, 2.0, 1.0, 0.5, 0.1
		x^2, y^2, z^2	1.0, 0.5
	O_2	s	4.0, 2.0, 1.0, 0.5, 0.1
		xz	2.0, 1.0, 0.5, 0.1
ka_2	O_1	xy	4.0, 2.0, 1.0, 0.5, 0.1, 0.05, 0.01
	O_2	y	6.0, 2.0, 1.0, 0.5, 0.1, 0.05
kb_1	O_1	y	8.0, 4.0, 2.0, 1.0, 0.5, 0.1, 0.05
		yz	2.0, 1.0, 0.5, 0.1, 0.05
	O_2	y	2.0, 1.0, 0.5, 0.1, 0.05
kb_2	O_1	x	8.0, 4.0, 2.0, 1.0, 0.5, 0.1, 0.05
		xz	2.0, 1.0, 0.5, 0.1, 0.05
	O_2	s	6.0, 2.0, 1.0, 0.5, 0.1
		x	2.0, 1.0, 0.5, 0.1
		z	2.0, 1.0, 0.5, 0.1

[a] Cartesian Gaussian basis functions are defined as
$\phi^{\alpha,\ell,m,n,\boldsymbol{A}}(\boldsymbol{r}) = N(x-\boldsymbol{A}_x)^{\ell}(y-\boldsymbol{A}_y)^{m}(z-\boldsymbol{A}_z)^{n}\exp(-\alpha|\boldsymbol{r}-\boldsymbol{A}|^2)$
with N a normalization constant.

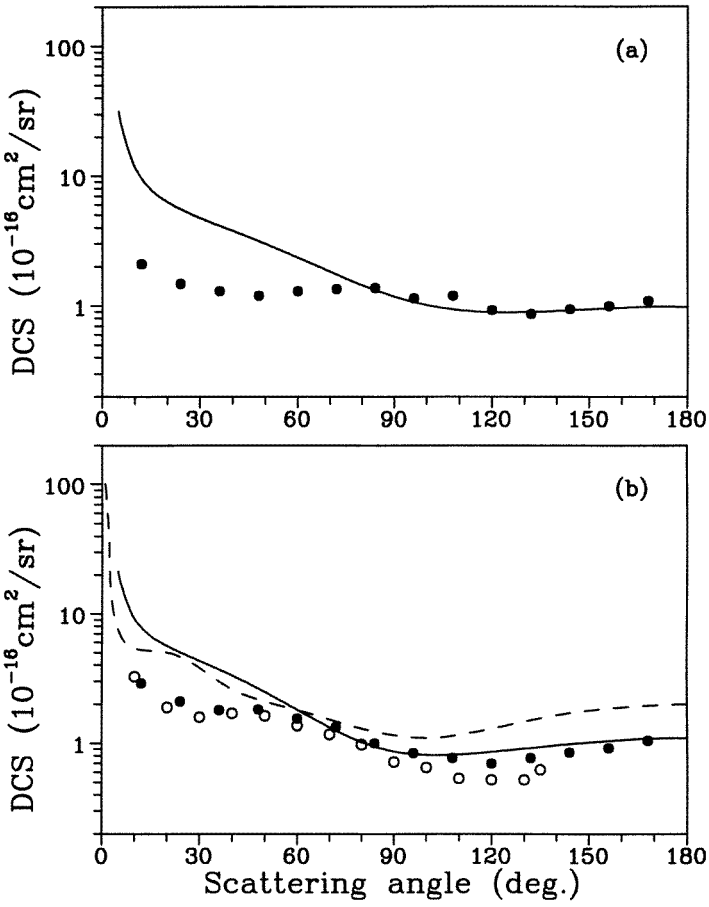

Figure 1. Differential cross sections for elastic e^-–O_3 scattering at (*a*) 3 eV and (*b*) 5 eV incident energies. Full curve: present calculated results; broken curve: calculated results of Okamoto and Itikawa (1993); full circles: experimental data of Shyn and Sweeney (1993); open circles: experimental data of Allan *et al* (1996).

where $X_{lh}^{p\mu}(\hat{r})$ are the generalized spherical harmonics (Burke *et al* 1972), related to the usual Y_{lm} by:

$$X_{lh}^{p\mu}(\hat{r}) = \sum_m b_{lhm}^{p\mu} Y_{lm}(\hat{r}). \tag{5}$$

Here p is an irreducible representation (IR) of the molecular point group, μ is a component of this representation and h distinguishes between different bases of the same IR corresponding to the same value of l. The coefficients $b_{lhm}^{p\mu}$ satisfy important orthogonality conditions and are tabulated in Burke *et al* (1972). To proceed, a set of L^2 functions is used to represent the initial trial scattering wavefunction. In this work, a set of Cartesian Gaussian basis functions, R_0, is chosen for this purpose. Improvement of the scattering wavefunctions can be achieved via an iterative procedure (Lucchese *et al* 1982). The method consists basically of augmenting the basis set R_0 by the set of partial-wave components $\tilde{\Psi}_{k,lh}^{(\pm)^{p\mu}}(\vec{r})$ of equation (4), where the sum in l is truncated to some cut-off value l_c. The new (augmented) set, R_1, is now used as a new basis for obtaining improved wavefunctions. This procedure can be continued until converged $\Psi_{k,lh}^{(+)^{p\mu}}(\vec{r})$ are obtained. These converged

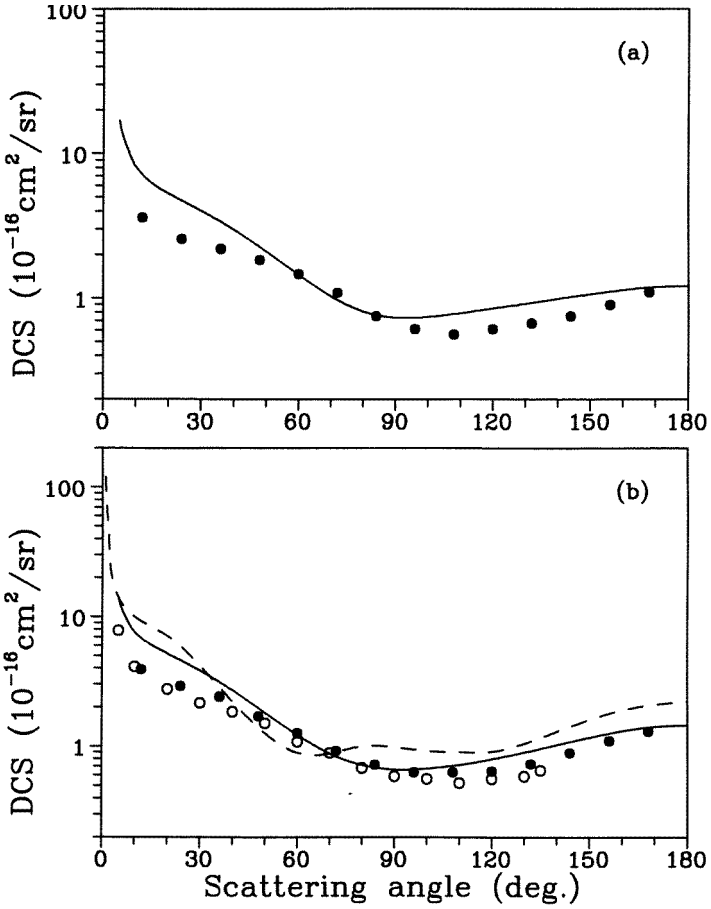

Figure 2. Differential cross sections for elastic e^-–O_3 scattering at (*a*) 7 eV and (*b*) 10 eV incident energies. The symbols used are the same as in figure 1.

scattering wavefunctions correspond, in fact, to exact solutions of the truncated Lippmann–Schwinger equation with SE potential (Lucchese *et al* 1980).

In this study, the higher partial-wave contributions are taken into account via a Born-closure procedure which is the same as that recently used by our group (Machado *et al* 1995b) and by Rescigno and Lengsfield (1992) for the study of the elastic scattering of electrons by water. Different from the procedure adopted by Okamoto and Itikawa (1993), our Born-closure correction was applied directly on the T-matrix according to the formula:

$$T = T^B + \frac{1}{k}\sum_{p\mu lhl'h'}^{LL'} \mathrm{i}^{l-l'}(T^{p\mu^{SVIM}}_{k,lh;l'h'} - T^{p\mu^B}_{k,lh;l'h'})X^{p\mu}_{lh}(\hat{k})X^{p\mu^*}_{l'h'}(\hat{k}_0) \tag{6}$$

where $T^{p\mu^{SVIM}}_{k,lh;l'h'}$ are the partial-wave T-matrix elements calculated via SVIM and truncated to some cut-off values $L = (l_c, h_c)$ and $L' = (l'_c, h'_c)$, $T^{p\mu^B}_{k,lh;l'h'}$ are the corresponding partial-wave point-dipole Born T-matrix elements and T^B is the complete point-dipole Born T-matrix. In order to evaluate the DCS, T^B is calculated directly in LF. The summation in equation (6) is also written in LF by using usual transformations (Edmonds 1960).

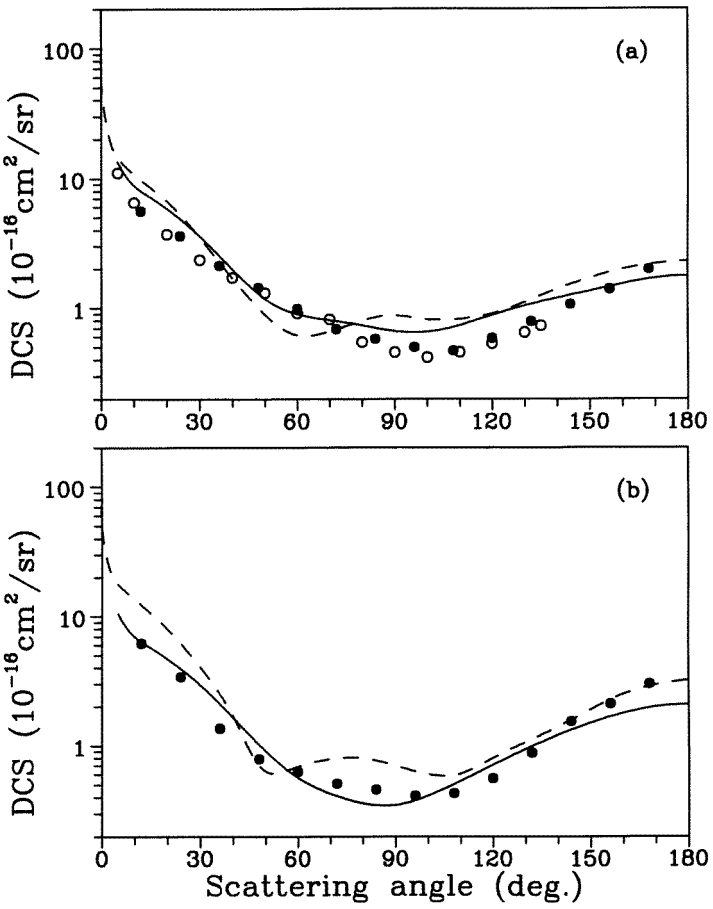

Figure 3. Differential cross sections for elastic e^-–O_3 scattering at (*a*) 15 eV and (*b*) 20 eV incident energies. The symbols used are the same as in figure 1.

The electronic configuration of the ground state O_3 is $1a_1^2 2a_1^2 3a_1^2 4a_1^2\ 5a_1^2 6a_1^2 1b_1^2\ 1b_2^2 2b_2^2 3b_2^2 4b_2^2\ 1a_2^2$, X^1A_1. The SCF wavefunction which is used to generate the SE potential is derived from a standard [11s6p/5s4p] Cartesian Gaussian basis set (Dunning 1971), augmented by three s ($\alpha = 0.0830$, 0.0237 and 0.006 71), one p ($\alpha = 0.0537$) and two d ($\alpha = 1.595$ and 0.371) uncontracted functions on the oxygen centres and four s ($\alpha = 9.281$, 2.327, 0.583 and 0.1457), three p ($\alpha = 5.21$, 1.33 and 0.4433) and one d ($\alpha = 1.423$) on the centre of mass. At the experimental equilibrium geometry ($R_{O-O} = 2.403\,97a_0$ and $\theta_{O-O-O} = 116.783^\circ$) (Maroulis 1992) this basis set gives an SCF energy of -224.323 au and an electric dipole moment of 0.362 au. These values are in good agreement with those calculated by Okamoto and Itikawa (-224.3286 au and 0.34 au) and by Sarpal *et al* ($-224.327\,97$ au and 0.33 au) as well as with the near-Hartree–Fock dipole moment (0.310 41) obtained by Maroulis (1992). The experimental dipole moment is 0.21 au (Mack and Muenter 1977).

In this study, the target bound orbitals are single-centre expanded about the centre of mass. This expansion is truncated at $l_c = 23$, all the possible values of $h \leqslant l$ are retained. The l_c for the expansion of the static potential is also taken as 23. In SVIM calculations,

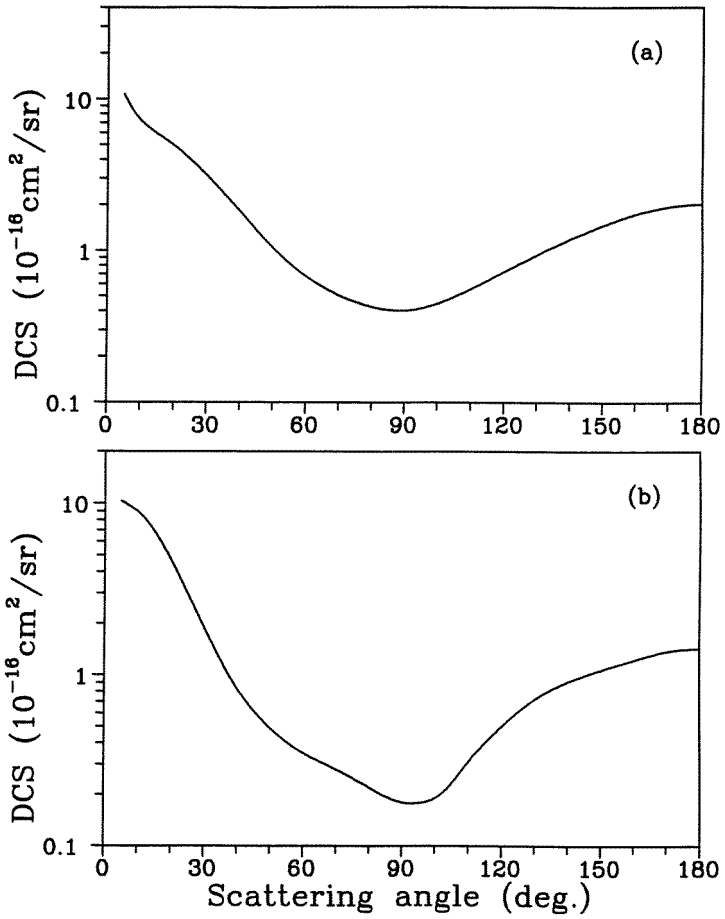

Figure 4. Differential cross sections for elastic e^-–O_3 scattering at (*a*) 30 eV and (*b*) 50 eV incident energies. Full curve: present calculated results.

we have limited the partial-wave expansion up to $l_c = 16$ for continuum orbitals of each symmetry as well as for all matrix elements appearing in these calculations. In addition, the radial integrals appearing in these calculations are evaluated using a Simpson quadrature.

In table 1 we show the basis set $\mathbb{R}_0$ used in the calculation of the initial trial scattering functions. All the SVIM calculations are converged within four iterations.

3. Results and discussion

In this investigation, cross sections were calculated in the 3–80 eV range. For incident energies $E_0 \leqslant 25$ eV, calculations were carried out at intervals of 1 eV. In figures 1–4 we show some selected results of our calculated DCS for e^-–O_3 scattering in the 3–50 eV incident energy range along with the experimental data of Shyn and Sweeny (1993) and of Allan *et al* (1996) as well as the theoretical results of Okamoto and Itikawa (1993) at the energies where they are available. As expected for electron scattering by polar molecules in the fixed-nuclei approximation, the calculated DCS diverge in the forward direction. In general, our results are in qualitative agreement with the experimental data in the entire

energy range. Quantitatively good agreement is also seen between our calculated DCS and the measured data for incident energies $E_0 \geqslant 7$ eV. At lower energies, however, our method overestimates the DCS for scattering angles $\theta \leqslant 60^\circ$. The discrepancies are probably due to the polarization effects which are not accounted for in this study. Although in our previous studies of elastic electron scattering by strongly polar molecules, such as H_2S (Machado *et al* 1995a) and H_2O (Machado *et al* 1995b) we have found that the polarization effects are less important than the target permanent dipole contributions, the dipole moment of O_3 is relatively small and thus target polarization may still play an important role for e^-–O_3 scattering in the low-energy range.

In relation to the calculated data of Okamoto and Itikawa (1993), although polarization effects were accounted for in their calculation, our results agree better with the measured data at all incident energies where comparisons are made. The good qualitative agreement between our calculated results with $l_c = 16$ and the measured data shows that the oscillations seen in the DCS curves of Okamoto and Itikawa (1993) are unphysical. In order to clarify

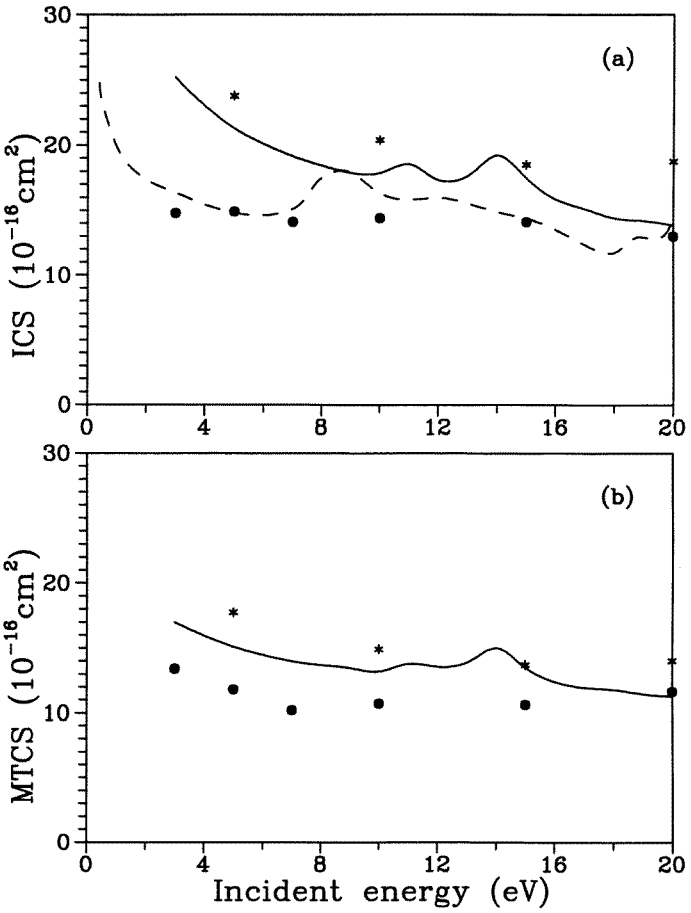

Figure 5. (*a*) Integral and (*b*) momentum transfer cross sections for elastic e^-–O_3 scattering for energies below 20 eV. Full curve: present calculated results; broken curve: calculated results of Sarpal *et al* (1994); stars, calculated results of Okamoto and Itikawa (1993); full circles, experimental data of Shyn and Sweeney (1993).

the nature of the oscillations, we have carried out a test run in which DCS at 20 eV were calculated using the same truncation parameter of Okamoto and Itikawa ($l_c = 8$) for the scattering wavefunction. The resulted DCS are similar to our results with $l_c = 16$ and do not show oscillations. Thus, our study seems to indicate that the oscillations seen in Okamoto and Itikawa's work is due to the Born-closure procedure used by these authors to take into account the contributions of higher angular-momentum components.

It is well known that the integral cross sections for electron–polar molecule scattering calculated using the fixed-nuclei approximation diverge at all incident energies. Nevertheless, in order to make a comparison with the calculated ICS of Sarpal *et al* (1994), we have calculated the ICS using only the truncated T-matrix elements obtained by SVIM according to the formula:

$$\sigma = \frac{4\pi}{k^2} \sum_{p\mu lhl'h'}^{LL'} |T_{k,lh;l'h'}^{p\mu\,SVIM}|^2. \tag{7}$$

Our calculated results in the 3–20 eV energy range are shown in figure 5(*a*) along with the experimental data of Shyn and Sweeny (1993) and the calculated ICS of Okamoto and Itikawa (1993) and Sarpal *et al* (1994). In figure 5(*b*), we compare our MTCS in the same energy range with the experimental data of Shyn and Sweeny (1993) and the calculated results of Okamoto and Itikawa (1993). In general, the agreement between our ICS and MTCS and the experimental results is fair and the results of Okamoto and Itikawa (1993) lie systematically above our results. On the other hand, the calculated data of Sarpal *et al* (1994) are about 10–20% lower than ours. Since our calculation as well as that of

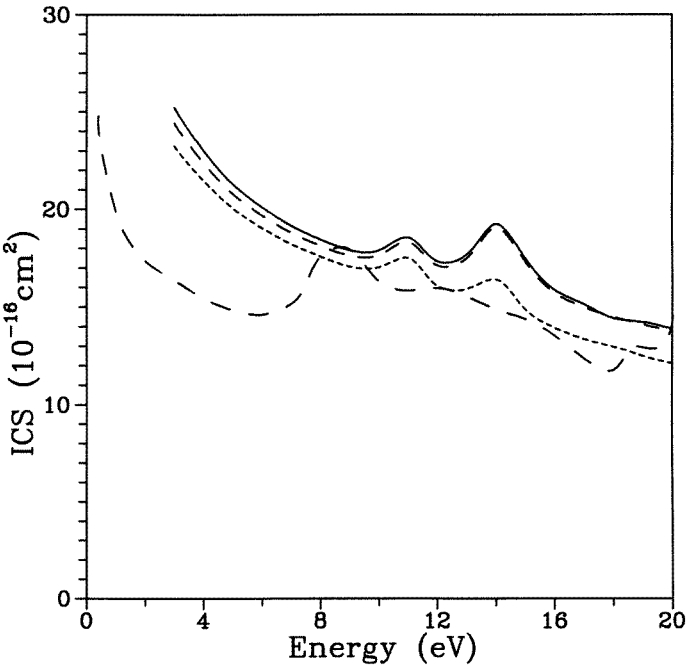

Figure 6. Integral cross sections for elastic e^-–O_3 scattering for energies below 20 eV. Full curve: present calculated results with $l_c = 16$; short broken curve: present calculated results with $l_c = 3$; broken curve: present calculated results with $l_c = 8$; long broken curve: calculated results of Sarpal *et al* (1994).

Sarpal *et al* were both performed at exact SE level, such difference is surprising and needs explanation. Also, the discrepancies cannot be attributed to the differences in the target representation since the calculated total energy and the dipole moment in both calculations agree very well with each other. Thus, the difference seen in ICS could possibly originate from the different truncation parameters used in the partial-wave expansions: $l_c = 3$ in theirs and $l_c = 16$ in ours. In order to clarify this point, in figure 6 we compare the ICS calculated with $l_c = 3$, 8 and 16 with those of Sarpal *et al* (1994). Our calculated ICS with $l_c = 3$ lie, in general, 10–17% below those with $l_c = 16$ and agree quite well with those of Sarpal *et al* for incident energies above 8 eV. Nevertheless, at lower energies, the results of Sarpal *et al* show a broad minimum in the 2–6 eV range which is seen neither in ours nor in Okamoto and Itikawa's calculations. We are unable to explain this difference in the low-energy range. In addition, our calculated ICS with $l_c = 8$ agree with those using $l_c = 16$ within 2% in average. Therefore, we estimate that our ICS with $l_c = 16$ are converged to better than 1%. Although the calculated ICS of Sarpal *et al* (1994) are in apparently better agreement with the measured results of Shyn and Sweeny (1993), this good agreement may be fortuitous since in there calculations only the contributions up to $l = 3$ were accounted for.

Moreover, our ICS and MTCS clearly show two resonance features at around 11 and 14 eV incident energies. Neither the measured data nor the calculated results of Okamoto and Itikawa (1993) give proof of such resonance structures. This is possibly due to the fact that both calculations and measurements were performed in a sparse energy mesh. On the other hand, the calculated ICS of Sarpal *et al* (1994) show

Table 2. Differential, integral and momentum-transfer cross sections (in 10^{-16} cm^2) for e^-–O_3 elastic scattering.

	E_0 (eV)									
Angle (deg)	3	5	7	10	15	20	30	40	50	80
5	31.70	21.40	16.96	13.94	13.51	10.43	8.90	11.00	10.30	15.50
10	11.56	9.16	8.09	7.60	8.83	6.94	7.22	7.84	8.91	10.45
20	6.29	5.61	5.27	5.19	5.87	4.69	4.57	4.55	4.65	4.16
30	4.74	4.30	4.01	3.82	3.59	2.93	2.43	2.11	1.89	1.35
40	3.78	3.32	2.98	2.69	2.00	1.66	1.20	0.95	0.83	0.71
50	3.01	2.48	2.11	1.81	1.18	0.91	0.68	0.53	0.49	0.50
60	2.35	1.81	1.46	1.22	0.90	0.57	0.45	0.38	0.35	0.38
70	1.84	1.33	1.03	0.88	0.81	0.43	0.32	0.30	0.28	0.32
80	1.45	1.02	0.81	0.72	0.74	0.36	0.22	0.22	0.22	0.30
90	1.19	0.87	0.73	0.66	0.67	0.35	0.19	0.19	0.18	0.29
100	1.02	0.81	0.74	0.67	0.66	0.41	0.23	0.19	0.19	0.25
110	0.93	0.82	0.79	0.72	0.74	0.53	0.34	0.29	0.31	0.24
120	0.90	0.86	0.85	0.80	0.89	0.71	0.54	0.50	0.50	0.28
130	0.90	0.92	0.92	0.90	1.04	0.94	0.83	0.77	0.72	0.36
140	0.92	0.97	0.99	1.03	1.20	1.21	1.24	1.08	0.91	0.46
150	0.95	1.02	1.07	1.17	1.35	1.50	1.69	1.39	1.07	0.57
160	0.97	1.06	1.14	1.31	1.54	1.79	2.12	1.67	1.22	0.67
170	0.99	1.09	1.20	1.42	1.70	2.00	2.45	1.90	1.37	0.77
180	0.99	1.10	1.21	1.45	1.77	2.08	2.52	1.95	1.42	0.83
ICS[a]	25.22	21.28	19.14	17.88	17.48	13.84	12.11	10.94	10.32	8.98
MTCS	16.17	14.81	13.83	13.08	13.39	11.09	10.04	8.57	7.36	4.98

[a] ICS are calculated using equation (7).

a resonance structure at around 9 eV and some oscillations in the 17–20 eV range. The authors have attributed the structures in the ICS to shape resonances in both the A_1 (at 8.2 and 18.0 eV) and B_2 (at 11.1 and 18.1 eV) irreducible representations and also one resonance in the A_2 representation (at near 20 eV). In order to characterize the resonances seen in our calculation, in figures 7(*a*) and (*b*) we show the calculated partial eigenphase sums for the ka_1 and kb_2 scattering channels in the 3–20 eV range, respectively. The corresponding data of Sarpal *et al* (1994) are also shown for comparison. Jumps in our calculated eigenphase sums at around 11 eV for ka_1 (figure 7(*a*)) and at around 14 eV for kb_2 (figure 7(*b*)) scattering channels are clearly seen. Therefore, the structures at around 11 eV in both ICS and MTCS is of ka_1 nature whereas those seen at around 14 eV is of kb_2 nature. Our assignment is in agreement with that of Sarpal *et al* although the positions of the resonances in this study are shifted by about 3 eV to higher incident energies. However, the reason for this shift is not clear since it has been shown in figure 6 that different truncations in partial-wave expansion would not affect in the position of resonances. In contrast to Sarpal's study, our

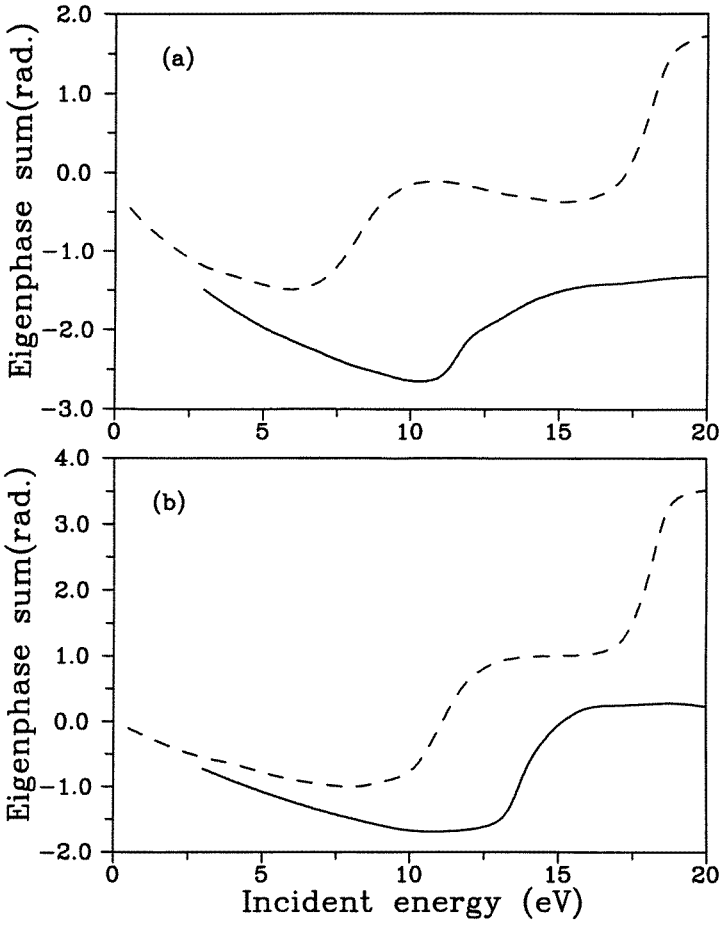

Figure 7. Eigenphase sums for the (*a*) ka_1 and (*b*) kb_2 scattering channels for elastic e^-–O_3 scattering. Full curve: present calculated results; broken curve: calculated results of Sarpal *et al* (1994).

calculation shows no evidence of resonances in the 17–20 eV energy range. Therefore, this study confirms that the resonances at higher energies seen by Sarpal *et al* are not real.

For the sake of completeness, calculated DCS, ICS and MTCS for some selected energies are presented in table 2.

Therefore this work reports a point-dipole Born-closure SE study for the elastic electron–ozone scattering in the 3–80 eV range. Our calculated DCS are in general good agreement with the available experimental data for incident energies $E_0 \geqslant 7$ eV. At lower energies, some discrepancies are seen at small scattering angles which can probably be attributed to the target polarization effects, not accounted for in this study. Moreover, our study shows that the oscillations in the DCS curves reported by Okamoto and Itikawa (1993) are unphysical which is probably originated by the Born-closure procedure used in their calculation. In addition, our study confirms the existence of some resonances reported by Sarpal *et al* (1994) although located at different positions. The reason of this discrepancy is not clear since different truncations in partial-wave expansion would not affect the position of resonances.

Acknowledgments

This work is partially supported by Brazilian agencies FINEP-PADCT, CAPES-PADCT, CNPq and FAPESP.

References

Allan M, Asmis K R, Popovic D B, Stepanovic M, Mason N J and Davies J A 1996 *J. Phys. B: At. Mol. Opt. Phys.* **29** 4727

Andersson K, Borowski P, Fowler P W, Malmqvist P-Å, Roos B O and Sadlej A J 1992 *Chem. Phys. Lett.* **190** 367

Burke P G, Chandra N and Gianturco F A 1972 *J. Phys. B: At. Mol. Phys.* **5** 2212

Celotta R J, Mielczarek S R and Kuyatt C E 1974 *Chem. Phys. Lett.* **24** 428

Dunning T H 1971 *J. Chem. Phys.* **55** 716

Edmonds A R 1960 *Angular Momentum and Quantum Mechanics* (Princeton, NJ: Princeton University Press)

Eliasson B, Kogelschatz U, Strassler S and Hirth M 1983 *Browm Boveri Research Report No. KLR-83-28C*

Johnstone W M, Mason N J, Newell W R, Biggs P, Marston G and Wayne R P 1992 *J. Phys. B: At. Mol. Opt. Phys.* **25** 3873

Lucchese R R, Raseev G and McKoy V 1982 *Phys. Rev.* A **25** 2572

Lucchese R R, Watson D K and McKoy V 1980 *Phys. Rev.* A **22** 421

Machado L E, Leal E P, Lee M T and Brescansin L M 1995a *Theochem.* **335** 37

Machado L E, Mu-Tao L, Brescansin L M, Lima M A P and McKoy V 1995b *J. Phys. B: At. Mol. Opt. Phys.* **28** 467

Mack K M and Muenter J S 1977 *J. Chem. Phys.* **66** 5278

Maroulis G 1992 *J. Phys. B: At. Mol. Opt. Phys.* **25** L77

Okamoto Y and Itikawa Y 1993 *Chem. Phys. Lett.* **203** 61

Rescigno T N and Lengsfield B H 1992 *Z. Phys.* D **24** 117

Sarpal B K, Pfingst K, Nestmann B M and Peyerimhohh S D 1994 *Chem. Phys. Lett.* **230** 231

Shyn T W and Sweeney C J 1993 *Phys. Rev.* A **47** 2919

Siegel M W 1982 *Int. J. Mass Spectrom.* **44** 19

Swanson N and Celotta R J 1975 *Phys. Rev. Lett.* **35** 783